

# Explosive Common-Envelope Ejection: Implications for Gamma-Ray Bursts and Low-Mass Black-Hole Binaries

Philipp Podsiadlowski<sup>1\*</sup>, Natasha Ivanova<sup>2,3</sup>, Stephen Justham<sup>1,4</sup>, Saul Rappaport<sup>5</sup>

<sup>1</sup> *Dept. of Astronomy, Oxford University, Oxford, OX1 3RH, UK*

<sup>2</sup> *CITA, University of Toronto, 60 St. George, Toronto, ON M5S 3H8, Canada*

<sup>3</sup> *Department of Physics, University of Alberta, Edmonton, AB T6G 2G7, Canada*

<sup>4</sup> *Kavli Institute for Astronomy and Astrophysics, Peking University, Beijing 100871, China*

<sup>5</sup> *Department of Physics and Kavli Institute for Astrophysical Research, Massachusetts Institute of Technology, Cambridge, MA 02139*

6 November 2018

## ABSTRACT

We present a new mechanism for the ejection of a common envelope in a massive binary, where the energy source is nuclear energy rather than orbital energy. This can occur during the slow merger of a massive primary with a secondary of  $1 - 3 M_{\odot}$  when the primary has already completed helium core burning. We show that, in the final merging phase, hydrogen-rich material from the secondary can be injected into the helium-burning shell of the primary. This leads to a nuclear runaway and the explosive ejection of both the hydrogen and the helium layer, producing a close binary containing a CO star and a low-mass companion. We argue that this presents a viable scenario to produce short-period black-hole binaries and long-duration gamma-ray bursts (LGRBs). We estimate a LGRB rate of  $\sim 10^{-6} \text{ yr}^{-1}$  at solar metallicity, which implies that this may account for a significant fraction of all LGRBs, and that this rate should be higher at lower metallicity.

**Key words:** black holes – binaries: general – gamma-rays: bursts – stars: individual: X-ray Nova Sco – X-rays: stars.

## 1 INTRODUCTION

Roughly half of the known short-period black-hole binaries have low-mass companions (Lee, Brown & Wijers 2002). However, it has been realized for more than a decade now that such systems are difficult to form (see the discussion in Podsiadlowski, Rappaport & Han 2003 [PRH] and further references therein). The problem is that, in order to produce a short-period system (i.e.,  $\lesssim 15$  hrs) with a low-mass donor star, the progenitor system has to pass through a common-envelope (CE) phase where the binary’s period is reduced from a typical period of several years to less than a few days. In the standard model for CE evolution (Paczynski 1976), this requires that the orbital energy released in the spiral-in process is sufficient to eject the massive envelope of the primary. For a low-mass companion (i.e.,  $\lesssim 2 M_{\odot}$ ), this is energetically difficult, if not impossible, in particular considering the large binding energies of the massive envelope of the primaries (Dewi & Tauris 2001; PRH).<sup>1</sup>

This problem has led to the suggestion of a number of more exotic formation scenarios for low-mass black-hole binaries, e.g., involving a triple scenario (Eggleton & Verbunt 1986) or the formation of the companion from a disrupted envelope (Podsiadlowski, Cannon & Rees 1995; PRH). Alternatively, the low-mass black-hole binaries could descend from intermediate-mass systems (Justham, Rappaport & Podsiadlowski 2006), as is the case for the majority of low-mass neutron-star binaries (Pfahl, Rappaport & Podsiadlowski 2003). In this paper, we present a new mechanism for the ejection of the common envelope: “explosive common-envelope ejection”, involving nuclear rather than orbital energy, which can be highly efficient in ejecting a massive envelope even if the companion is a relatively low-mass star.

A particularly interesting black-hole binary is the well studied system GRO J1655–40 (Nova Scorpii 1994). It has an orbital period of 2.6 d and a black hole with a mass  $\sim 5.4 M_{\odot}$  (Beer & Podsiadlowski 2002). Israelian et al. (1999) claimed that the secondary in this system has been highly enriched with the products of explosive nucleosynthe-

\* E-mail: podsi@astro.ox.ac.uk

<sup>1</sup> In a recent study by Yungelson et al. (2006), as well as in some other studies, this problem did not seem to arise. However, these authors used a prescription for the binding energy of the envelope that *underestimates* the binding energy by up to a factor of 10

compared to the actual binding energies calculated from realistic models for the structure of massive supergiants (Dewi & Tauris 2001; PRH).

sis (e.g., Mg, Si, S, Ti) produced in the supernova explosion that produced the black hole.<sup>2</sup> Based on the actual abundance ratios, Podsiadlowski et al. (2002) found some tentative evidence that these are better explained by an energetic supernova explosion, a hypernova, with a typical ejecta energy of  $\gtrsim 10^{52}$  ergs (i.e., 10 times the energy in a ‘typical’ supernova). This may suggest that the formation of the black hole in this system could have been accompanied by a long-duration gamma-ray burst (LGRB). However, in this case it is puzzling why the black-hole progenitor would have been rapidly rotating as required in the collapsar model for LGRBs (Woosley 1993; MacFadyen & Woosley 1999) since the core of the primary should have been spun down rather than have been spun up during its evolution (Heger, Woosley & Spruit 2005). As we will show later in this paper, in the case of explosive CE ejection, this problem does not arise, possibly linking the formation of compact black-hole binaries having low-mass secondaries to LGRBs.<sup>3</sup>

This process of explosive CE was discovered in a systematic study of the slow merger of massive stars (Ivanova 2002; Ivanova & Podsiadlowski 2003; Ivanova & Podsiadlowski 2010), where it was found that, in some cases in the late stage of the spiral-in process, hydrogen-rich material could be mixed into the helium-burning shell leading to a thermonuclear runaway which released enough energy to eject both the hydrogen and the helium envelope (see Figure 1 for a schematic representation), possibly explaining why to date all supernovae associated with LGRBs appear to be Type Ic supernovae (i.e., supernovae without hydrogen and helium in their spectrum; cf. Podsiadlowski et al. 2004).<sup>4</sup>

In this paper, we will first discuss the numerical method in Section 2, and the physics of the process of explosive CE ejection in Section 3. In Section 4 we apply it to the formation of low-mass black-hole binaries and LGRBs, and end with a broader discussion in Section 5.

## 2 THE NUMERICAL CODE

To model the merging of the two stars, we used a modified one-dimensional Henyey-type stellar evolution code (based on Kippenhahn, Weigert & Hofmeister 1967), which has recently been updated (Podsiadlowski, Rappaport & Pfahl 2002). It uses OPAL opacities (Rogers & Iglesias 1992), supplemented by molecular opacities from Alexander & Fergu-

<sup>2</sup> In this context, we refer the reader to two related studies: one by Foellmi, Dall & Depagne (2007) challenging the original claim of these overabundances, and one by González Hernández, Rebolo & Israelian (2008) re-affirming them.

<sup>3</sup> Brown et al. (2000) were the first to suggest that the formation of the black hole in GRO J1655-40 was associated with an LGRB and proposed a general link between low-mass black-hole binaries and LGRBs (see, in particular, Brown, Lee & Moreno Méndez 2007). Similar to the present study, they suggest late Case C mass transfer for the progenitor systems, but argue for the spin-up of the cores rather than spin-down during the CE phase, invoking tidal locking, an assumption that remains to be proven.

<sup>4</sup> We note that Siess & Livio (1999a,b) were the first to point out the potential importance of nuclear energy on the CE ejection process in their modelling of the dissolution of planets/brown dwarfs in red-giant stars.

son (1994) at low temperatures and a mixing-length parameter  $\alpha = 2$ . Following the calibration by Schröder, Pols & Eggleton (1997) and Pols et al. (1997), we generally assume 0.25 pressure scale heights of convective overshooting, unless stated otherwise.

In the calculation of the spiral-in and merger phase we followed the angular-momentum transport in the envelope of the primary, using prescriptions similar to those given by Heger & Langer (1998), where the source of the angular momentum is the orbital decay of the immersed binary. This is important for determining the averaged distribution of the heating sources inside the common envelope. The envelope heating is provided by the dissipation of the kinetic energy of the differentially rotating shells due to viscous friction. Note that this energy is not necessarily released in the same place where the angular momentum has been deposited initially. For modelling the latter, we included a prescription that simulates the frictional energy input during the spiral-in phase of the companion star similar to the prescription given by Meyer & Meyer-Hofmeister (1979) (also see Podsiadlowski 2001).

Once the immersed secondary fills its own critical potential surface (i.e., its equivalent ‘‘Roche lobe’’ defined by the effective potential of the core-secondary pair) within the common envelope, we simulate the mass transfer guided by the detailed stream-core simulations presented in Ivanova, Podsiadlowski & Spruit (2002). We use their equation (28) to determine the depth to which the stream penetrates the hydrogen-exhausted core of the primary and vary the parameter  $k$  to take into account uncertainties in the modelling of the stream-core impact.<sup>5</sup>

In each time step, we determine how much mass is lost from the secondary and deposit this material with the appropriate entropy at the bottom of the stream. In this phase, the mass-transfer rate from the secondary is still determined by the frictional angular-momentum loss the immersed binary experiences, and reaches up to  $100 M_{\odot} \text{ yr}^{-1}$  in the final phase.

Since hydrogen is deposited in layers with temperatures  $T > 10^8$  K, an extended nuclear reaction network, including all important weak interactions, is included using the REACLIB library (Thielemann, Truran & Arnould 1986). This library provides the data for reaction rates which can be applied for a wide range of temperatures ( $T = 10^7 - 10^{10}$  K) for all elements up to  $^{84}\text{Kr}$ . For heavier elements, the library has been updated for neutron-capture cross-sections and half-lives of beta-decays for the s-elements from  $^{85}\text{Rb}$  up to  $^{209}\text{Bi}$ . The data for these cross-sections were taken from the work of Beer, Voss and Winters (1992) and have been interpolated using the method of minimal squares to fit the formulae for reaction rates used in REACLIB. The data for the half lives of the beta-decays were taken from Newman (1978). We note that, in explosive phases, the nuclear timescales of many reactions are shorter than the convective turnover timescales in convective regions, and thus the

<sup>5</sup> The parameter  $k$  defines the stream penetration efficiency and depends on the amount of entropy that is generated in the stream-core impact: a larger  $k$  corresponds to the case where the ambient medium near the core has a larger pressure and temperature gradient resulting in the generation of stronger shocks and faster dissipation of the stream.

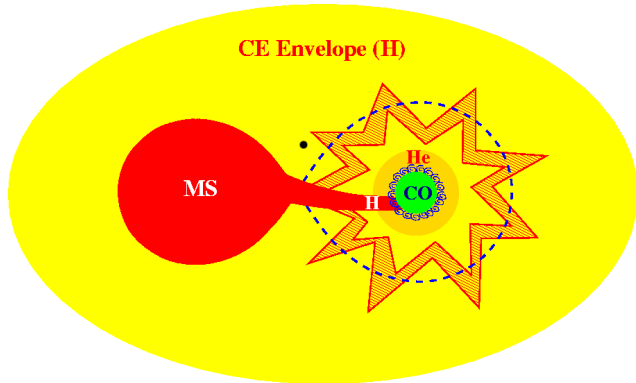


**Figure 1.** Schematic illustration of the process of explosive common-envelope ejection. The H-rich stream from the Roche-lobe-filling immersed companion penetrates deep into the core of the primary, mixing hydrogen into the helium-burning shell. This leads to a thermonuclear runaway ejecting both the helium shell and the hydrogen-rich envelope and leaving a bare CO core.

assumption of homogeneous mixing in the convective layers is not valid. To treat the time-dependent nuclear burning in convective zones, we therefore use a modified version of the two-stream formalism developed by Cannon (1993).<sup>6</sup>

### 3 EXPLOSIVE MERGING AND COMMON-ENVELOPE EJECTION

#### *The case of an $18 M_{\odot}$ primary*

To explore the conditions for explosive common-envelope ejection, we performed a detailed numerical study of the merger of a  $18 M_{\odot}$  primary with secondaries in the range of  $1-5 M_{\odot}$ . In all cases, we assumed that the spiral-in phase started when the primary had completed helium core burning and was ascending the red-supergiant branch for the second time (so-called Case C mass transfer; Lauterborn 1970). Figure 2 shows the results of a typical calculation which illustrates the evolution from the initial spiral-in phase to the point at which the envelope is ejected. To test the effects of convective overshooting, we used models with 0.25 pressure scale heights of convective overshooting and models without convective overshooting, where the former produces a H-exhausted core of  $6.8 M_{\odot}$ ,  $1.3 M_{\odot}$  larger than the latter. To examine the uncertainties due to the modelling of the stream-core interaction, we use two different parameters for the entropy generation in equation (28) of Ivanova et al. (2002),  $k = 0.2$  for low-entropy generation and  $k = 0.4$  for high-entropy generation. We note that, in the present study, we did not model how rotation of the core affects the penetration depth (see section 5.3.2 of Ivanova et al. [2002]) and how this changes during the stream-core interaction phase. We do not expect that this would change our conclusions significantly.

#### *The initial set-up at the start of the merger*

At the end of the spiral-in, when the secondary starts to fill its Roche lobe within the common envelope, the secondary itself is located partially within the outer convective zone (OCZ) of the primary, although the inner Lagrangian point,  $L_1$ , is within the radiative zone. The layer of envelope material at the position of the secondary has expanded because of the frictional energy input from the spiral-in and has a density roughly two orders of magnitude less than before the spiral-in, with a typical range from about  $10^{-7} \text{ g cm}^{-3}$  to about  $10^{-5} \text{ g cm}^{-3}$ . The spiral-in does not affect the structure of the primary's core (the CO core plus the surrounding He shell), it only affects the structure of the radiative hydrogen zone between the OCZ and the He shell ( $\Delta M_{\text{H,rad}}$ ), since the upper part of this zone has been heated and may have become convective. For example, in the case of a  $5 M_{\odot}$  donor inside an  $18 M_{\odot}$  primary, the total mass of the OCZ is increased by  $0.4 M_{\odot}$ , while, in the case of a  $2 M_{\odot}$  donor, it is only increased by  $0.04 M_{\odot}$ . It should be noted that, in the first case, the initial  $\Delta M_{\text{H,rad}}$  is  $0.13 M_{\odot}$  for our standard case with convective overshooting. Without convective overshooting, it would be  $0.7 M_{\odot}$ . The corresponding radial sizes of this zone ( $\Delta R_{\text{H,rad}}$ ) are  $1.6 \times 10^{11} \text{ cm}$  and  $2.5 \times 10^{11} \text{ cm}$  for the case with and without convective overshooting, respectively.

#### *The stream behavior and the surrounding medium*

Once the stream leaves the secondary, the depth of its penetration depends on the initial entropy of the stream material and on how much this entropy is modified during the stream's penetration into the primary's core by shocks (Ivanova et al. 2002). The latter is a function of the density contrast between the stream and the surrounding matter and depends on how strongly the medium itself is stratified. A larger density gradient in the primary's material near the stream leads to more entropy generation in the stream. The stream will stop its fall when the ambient pressure becomes comparable to the stream pressure.

In the test cases, the penetration depth is two times smaller in the model with large entropy generation (with  $k = 0.4$ ) than in the model with  $k = 0.2$ . The distance to the He shell from  $L_1$  is also larger. For a secondary that is more massive than  $\sim 3 M_{\odot}$ , the stream is unable to penetrate into the He shell since the density contrast between the stream and the ambient medium is lower and the stream entropy higher.

#### *The response of the He shell to the injection of hydrogen*

In the layer where the hydrogen-rich stream penetrates into the helium-dominated layer (see the middle and right panels of Figure 2), the stream entropy is higher than that of the surrounding material. As a consequence, both the entropy and the hydrogen mass fraction  $X$  have negative gradients. This leads to the formation of a local convective zone that rapidly expands outwards. As the stream continues to hit the core, it penetrates progressively deeper into the core for several reasons: first, the entropy of the donor material decreases as material from deeper inside the star is transferred.

<sup>6</sup> Further details of the code can be found in Ivanova (2002) and in Ivanova & Podsiadlowski (2010).

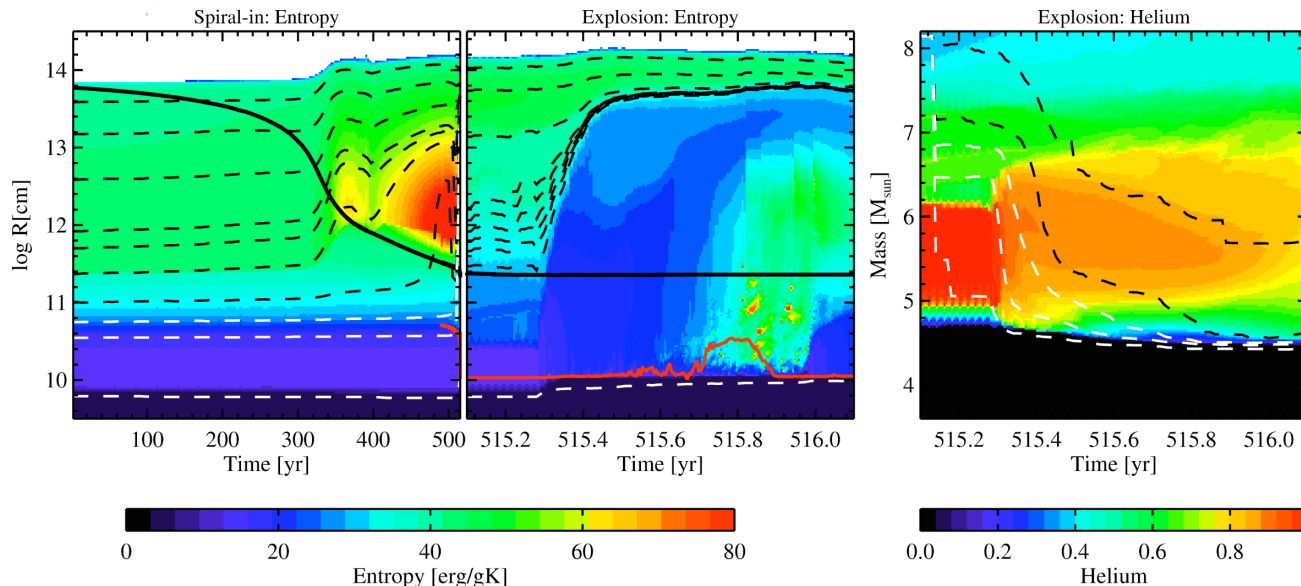


**Figure 2.** Simulations of the spiral-in of a  $2 M_{\odot}$  star inside the envelope of a  $18 M_{\odot}$  red supergiant (after He core burning) up to the phase where the H/He envelope is being ejected. The left and medium panels show the time-evolution of the specific entropy profile as a function of radius; *left panel*: from the start of the spiral-in up to the beginning of the He shell explosion phase; *middle panel*: during the final year around the He shell explosion. The right panel shows the time-evolution of the helium profile as a function of mass during the last year. The black solid curve in the left and medium panels shows the orbital position of the secondary, the solid red curves show the depth of the stream penetration. The dashed curves are curves of constant mass and correspond to  $M = 14, 9, 7.30, 6.92, 6.88, 6.84, 6.80, 6.72, 4.457 M_{\odot}$  (from the top). The dashed curves in the right panel are curves of constant radii and correspond to  $\log R/\text{cm} = 13.6, 13, 12, 11, 10$  (from the top). The stream penetration efficiency parameter for this model is  $k = 0.2$ .

Second, the outer layer of the He shell starts to expand, reducing the density in the outer part of the He shell. Third, the mass transfer rate steadily goes up, and, fourth, the  $L_1$  point moves closer to the helium core. In the case where the initial stream does not penetrate deeply enough into the He-rich layer and is unable to create a negative entropy gradient in the ambient medium, a convective zone still develops in the region where the stream is being dissolved, but more slowly (the stream’s entropy is still higher than the ambient medium and stream energy is being deposited, further increasing the entropy). This convective zone propagates inwards as the stream penetrates deeper. We found that in some models this zone can connect with the OCZ; however, it either never penetrates deeply enough to connect to the convective helium-burning shell, or it starts efficient steady hydrogen burning, leading to a drop of the temperature in the He convective shell.

#### *The conditions for explosive CE ejection*

Based on these simulations, it seems that the main condition for experiencing explosive CE ejection (ECEE) is that the stream is able to penetrate deeply enough into the He-rich zone from the very beginning such that both a negative entropy and a negative composition gradient are created. This favours models with convective overshooting and low-entropy generation. It also favours lower-mass secondaries with lower entropies. For example, for  $M_2 = 2 M_{\odot}$ , after leaving  $L_1$ , the stream can penetrate as much as  $2.5 R_{\odot}$  of the core, while for  $M_2 = 5 M_{\odot}$  it stops further from the

primary center, passing through only  $1 R_{\odot}$ . An alternative criterion is that  $\Delta M_{\text{H,rad}}$  is small:  $\Delta M_{\text{H,rad}} \leq 0.2 M_{\odot}$ .

Based on our test calculations, we conclude that the conditions for a successful explosive common-envelope ejection are satisfied for secondary masses up to  $3 M_{\odot}$  in the models with convective overshooting. A lower limit on the secondary mass is roughly given by  $1 M_{\odot}$  where the energy released in the spiral-in does not provide enough energy to lead to an expansion of the envelope (i.e. lead to a “slow” merger); in that case the merger is expected to occur on a dynamical timescale.

With these constraints to guide us, we find that the ECEE conditions are found for primaries with masses up to  $40 M_{\odot}$ . If the minimum mass for black-hole formation is  $25 M_{\odot}$ , this leads to CO cores in the range of  $6.5\text{--}13 M_{\odot}$  (using our standard convective overshooting parameter).

The amount of mass transferred from the secondary before the CE ejection also depends on the secondary’s mass: it is about  $1 M_{\odot}$  for a  $3 M_{\odot}$  secondary,  $0.8 M_{\odot}$  for a  $2 M_{\odot}$  secondary and  $0.2\text{--}0.3 M_{\odot}$  for a  $1 M_{\odot}$  secondary (but this depends somewhat on the stream entropy parameter).

#### *The final stage*

While the initial spiral-in and the early merger phase take place on a timescale of  $\sim 100$  yr, once the H-rich stream connects to the helium-core-burning shell, the evolution accelerates. The overall duration of the explosive phase is  $\sim 1/4$  yr, although 90% of the energy is released in the last few days. At the end of our calculations, the outer parts of the core expand with a velocity exceeding the local escape velocity,

and typically  $0.03\text{--}0.06 M_{\odot}$  of stream material has been burned explosively. The nuclear energy that has been released ( $\gtrsim 2 \times 10^{50}$  ergs) exceeds the binding energy of both the He-rich layer and the common envelope by about a factor of 2.

By the time the envelope is ejected, we find that the CO core has been moderately spun-up by the accretion of angular momentum and transport into the core during the pre-explosive core-accretion phase. The characteristic specific angular momentum of the core is  $\sim 10^{16} \text{ cm}^2 \text{ s}^{-1}$ , at the low end of what is required in the collapsar model for LGRBs. However, further spin-up is possible, since even after the ejection of the envelope, mass transfer is likely to continue and the system is close enough for tidal spin-up to operate.<sup>7</sup>

Indeed, despite the ejection of the helium shell, the system does not widen appreciably, if at all, because there is still enough frictional angular-momentum loss to keep the secondary in Roche-lobe contact. This suggests that the system will continue to transfer mass after the CE ejection.<sup>8</sup> This mass transfer occurs on a thermal timescale since the secondary is highly out of thermal equilibrium, in fact has a radius smaller than its equilibrium radius, and will try to expand towards a new thermal-equilibrium stage.

The remaining evolution of the primary's CO core to core collapse is expected to be of order a few  $10^3$  to at most  $10^4$  yr (in the  $18 M_{\odot}$  simulation it was 3000 yr). We note that this time is significantly longer than it would have taken the core to core collapse without the ejection of the He layer because of the significant core expansion and cooling.

#### 4 APPLICATION TO LGRBS AND SHORT-PERIOD BLACK-HOLE BINARIES

In order to assess the importance of ECEE events for LGRBs and low-mass black-hole binaries, we first estimate in this section the expected rate of these events and then present detailed binary population synthesis results that simulate the properties of the resulting black-hole (BH) binaries.

##### 4.1 The ECEE Rate

Using the results discussed in the previous section, it is straightforward to estimate the fraction of binaries that experience explosive CE ejection. This depends mainly on the secondary mass and the condition that the systems experience Case C mass transfer.

Figure 3 shows the cumulative rate for ECEE events

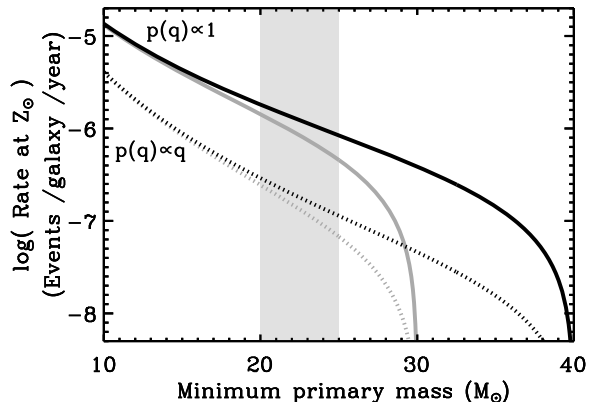


**Figure 3.** The cumulative rate for ECEE events as a function of the minimum primary mass required. The black curves assume a maximum primary mass of  $40 M_{\odot}$  whilst the grey curves take a maximum primary mass of  $30 M_{\odot}$ . The solid curves assume a flat initial mass-ratio distribution ( $p(q) = \text{constant}$ ), the dotted curves use  $p(q) \propto q$ . The light grey shading indicates a plausible range for the minimum mass of a single star which can form a black hole at solar metallicity. For these estimates we assumed that 1% of binaries have an orbital period that leads to Case C mass transfer. The actual rate could be higher by an order of magnitude at low metallicity, and the minimum mass for BH formation could be lower.

as a function of the minimum primary mass for different assumptions about the maximum mass of the primary and different mass-ratio distributions. Here, we assume that 1% of all binaries experience Case C mass transfer at solar metallicity. The primary masses  $M_1$  are chosen from an initial mass function  $p(M_1) \propto M_1^{-2.7}$  (Kroupa, Tout & Gilmore 1993). The rates are normalised to a core-collapse SN rate of 1 per century (i.e., assume that one star more massive than  $9 M_{\odot}$  is formed per century in a typical galaxy). This probably underestimates the core-collapse supernova rate in the Milky Way (Cappellaro, Evans & Turatto 1999). We also assumed that all massive stars form in binaries (Kobulnicky & Fryer 2007), with a distribution of initial separations  $a$  that is flat in  $\log a$  between 3 and  $10^4 R_{\odot}$ .

A significant source of uncertainty in the ECEE rates is the initial mass-ratio distribution  $p(q)$ , where  $q = M_2/M_1$  is the mass ratio and  $M_2$  is the mass of the secondary. In Figure 3 we consider a distribution where  $p(q) = \text{constant}$  and one where  $p(q) \propto q$ .

In using the ECEE mechanism to produce short-period black-hole X-ray binaries, we require the primary to form a BH. The light grey shading in Figure 3 indicates the expected minimum mass for black-hole formation, which is generally believed to be in the range of  $20\text{--}25 M_{\odot}$  (see, e.g., Fryer & Kalogera 2001 and further references in PRH). Black-hole formation is also generally assumed to be a requirement for the formation of LGRBs, though we note that rapid rotation at core-collapse for lower mass cores may lead to the formation of magnetars (e.g., Thompson & Duncan 1993; Akiyama et al. 2003). Magnetar formation has also been proposed as a channel for LGRBs (e.g., Wheeler, Höflich & Wang 2000; Burrows et al. 2007; Uzdensky & MacFadyen 2007; Bucciantini et al. 2008), which would increase

<sup>7</sup> Detmers et al. (2008) found that, in a sufficiently close He-star binary (with  $P_{\text{orb}} \lesssim 10$  h), the core can be spun up significantly on a timescale of  $\sim 10^4$  yr (also see Brown et al. 2007). However, unlike the case considered by Detmers et al. (2008), the remaining lifetime of the primary after case C mass transfer is short enough that wind mass loss will not cause significant widening of the system which would then tidally spin down the star again.

<sup>8</sup> We note, however, that there are enough uncertainties in our calculations that we cannot rule out that the secondary will be out of Roche-lobe contact after the CE ejection. This will ultimately require full three-dimensional stellar-structure calculations.

the potential LGRB event rate from this proposed mechanism. Because of the steepness of the primary mass function, the upper limit of  $40 M_{\odot}$  indicated by our hydrodynamic calculations is of lesser importance to the rates.

The fraction of binary systems that experience Case C mass transfer is strongly dependent on the metallicity and the assumptions about the wind-loss rate from the primary star (see Justham & Podsiadlowski 2010), but for  $Z=0.02$ , 1% is a reasonable estimate. On the other hand, if the Nieuwenhuijzen & de Jager (1990) wind-loss rates are correct, only primary stars with masses  $\lesssim 30 M_{\odot}$  can experience Case C mass transfer. This mass goes up to  $\simeq 40 M_{\odot}$  if the Nieuwenhuijzen & de Jager rate is reduced by a factor 1/3, to take into account that the empirical rates are not corrected for the effects of wind clumping (e.g., Moffat & Carmelle 1994; Fullerton, Massa & Prinja 2006). However, as Figure 3 shows, the uncertainty in this upper mass limit is not a significant contribution to the uncertainty in the ECEE rate.

Hence, if we only allow primary masses of  $25 M_{\odot} \leq M_1 \leq 40 M_{\odot}$  to produce LGRBs through the ECEE channel, and take  $p(q) = \text{constant}$ , we obtain a LGRB rate of  $\sim 10^{-6} \text{ gal}^{-1} \text{ yr}^{-1}$ . This is consistent, though at the lower end, of recent LGRB rate estimates (e.g., Podsiadlowski et al. 2004). There is some evidence that LGRBs prefer lower metallicity (e.g., Fruchter et al. 2006; Wolf & Podsiadlowski 2007; Modjaz et al. 2008). This is consistent with the ECEE scenario, since the rate of case C mass transfer increases with decreasing metallicity, by up to at least a factor of 10 at extremely low metallicity ( $Z \lesssim 0.0001$ ; Justham & Podsiadlowski 2010). Given the uncertainties in these estimates, we conclude that the ECEE channel could account for at least a significant subset of the LGRB rate and possibly all of it.

#### *Consistency between the LGRB rate and the short-period BH binary birthrate*

ECEE links LGRBs with short-period black-hole X-ray binaries. Wijers (1996) and Romani (1998) estimated the Galactic population of short-period BH XRBs to be at least  $\sim 1000$ . For a birthrate of  $\sim 10^{-6} \text{ gal}^{-1} \text{ yr}^{-1}$ , this requires a plausible mean system lifetime of  $\sim 1 \text{ Gyr}$ . This assumes that the majority of systems will not be disrupted by the supernova explosion and will reach Roche-lobe contact in a reasonable time. In the following subsection we simulate the properties of the predicted X-ray binary population from this channel.

## 4.2 Method & Assumptions

For the population synthesis calculation, we randomly selected a set of  $5 \times 10^5$  binaries with initial primary masses  $M_1$  between 25 and  $40 M_{\odot}$  and initial secondary masses  $M_2$  between 1 and  $3 M_{\odot}$ . We again adopted an initial mass function  $p(M_1) \propto M_1^{-2.7}$  and a flat mass-ratio distribution. After the CE ejection, the secondary is assumed to be filling its Roche lobe, although in reality it may be slightly underfilling it because of the mass loss associated with the CE ejection.

The core mass of the primary  $M_{\text{core}}$  can be related to the initial primary mass according to the simple estimate

$$(M_{\text{core}}/M_{\odot}) = 0.12 (M_1/M_{\odot})^{1.35}. \quad (1)$$

(Hurley et al. 2000). This yields post-ECEE remnant masses in the range of  $9.3 - 17.5 M_{\odot}$  for initial primary masses between 25 and  $40 M_{\odot}$ . The secondary, having lost mass during the CE phase, leaves a donor star of mass  $M_{\text{don}}$ , where

$$(M_{\text{don}}/M_{\odot}) = 0.2 + 0.6 (M_2/M_{\odot}) \quad (2)$$

(in accordance with the results in Sect. 3). The orbital period and component masses are assumed to be unchanged until the core explodes as a supernova. After the supernova, the core becomes a BH; we determine the mass of the BH using the results of Fryer & Kalogera (2001), as formulated in Belczynski et al. (2008).<sup>9</sup>

Mass loss from the system and any kick imparted to the black hole during the supernova will change the orbital period and eccentricity (see, e.g., Brandt & Podsiadlowski 1995; Kalogera 1996). We assume that the supernova kicks are randomly oriented, and sample the kick distributions assuming that it can be described by a Maxwellian distribution with a velocity dispersion  $\sigma_k$  (for a discussion of supernova kicks in the formation of black holes, see Brandt, Podsiadlowski & Sigurdsson 1995; PRH). We explored a range of values for  $\sigma_k$ , including zero kick velocity and kick velocities with the same kick *momentum* as found for single neutron stars (Hobbs et al. 2005).

If the system is not disrupted in the supernova, we assume that it circularises whilst conserving angular momentum. We also allow the system to survive even if the Roche-lobe radius of the donor star is as small as 90% of the ZAMS radius for the post-ECEE donor mass to take into account the fact that the secondary is likely to be still undersized and expanding at this stage, as indicated by our ECEE calculations. We assume that a short period of mass transfer driven by this expansion will increase the orbital period of the system until the star is in equilibrium, and assume, for simplicity, that the mass lost by the donor during that phase is negligible. The donor star is now assumed to be still essentially unevolved.

We weight the output of this algorithm by the initial mass function and initial mass-ratio distribution. This produces a probability distribution for the formation of post-supernova black-hole binaries. In order to simulate the population of black-hole X-ray binaries, we combine these formation probabilities with a grid of binary evolution sequences.

#### *Binary evolution grid*

To follow the X-ray binary phase, we calculated a grid of 936 binary evolution sequences using an updated version of Eggleton's stellar evolution code (e.g., Eggleton 1971; Pols et al. 1995) and a metallicity of 0.02. This grid was equally spaced in 13 donor masses ( $0.8$  to  $2.0 M_{\odot}$ ), 13 accretor masses ( $5$  to  $17 M_{\odot}$ ), and 12 values for the initial period. The first model is placed into contact at the start of its evolution, with an orbital period  $P_{\text{orb}} = P_{\text{ZAMS}}$ . The second begins in a binary with  $P_{\text{orb}}/P_{\text{ZAMS}}=1.1$ , and the remaining ten orbital periods are equally spaced in  $\log(P_{\text{orb}}/P_{\text{ZAMS}})$

<sup>9</sup> Specifically, their equations 1, 2 and 4.

between 0.1 and 1.0 (where  $P_{\text{ZAMS}}$  is the orbital period at which the donor is filling its Roche lobe when unevolved).<sup>10</sup>

The evolution of the systems is driven by angular-momentum loss. We include losses due to both gravitational wave radiation and magnetic braking, adopting the formalism of Ivanova & Taam (2003) for secondaries with  $M_2 < 1.5 M_\odot$  (see also Ivanova & Kalogera 2006). We consider only systems which reach contact before the end of the main sequence and have a maximum age for each system of 13 Gyr; we varied this maximum age and found it to have a relatively minor effect.

The formation probabilities produced by our population synthesis are all distributed among the eight members of the three-dimensional grid nearest to them, i.e. to a cube of gridpoints around each system, using trilinear interpolation to determine the weights attributed to each grid point. Each sequence in our binary evolution grid then possesses a formation likelihood, and the grid sequences are binned and combined in proportion to these formation probabilities. Within each sequence, the statistical weight of each evolutionary timestep is proportional to the duration of that timestep. This leads to a ‘steady-state’ X-ray binary population, assumed to be representative of the distribution in the Milky Way at the current epoch.

### 4.3 Results

Figure 4 shows a selection of our population synthesis calculations, which reproduces the shape of the observed orbital-period distribution fairly well, for  $\sigma_k = 200 \text{ km s}^{-1}$  and for no kick. However, the donor temperatures do not easily match the observations, unless either our model effective temperatures or our conversion from spectral type to effective temperatures is incorrect.

Note that these donor temperatures give a significantly better match to the observations than systems which initially contained intermediate-mass donors would provide (see, e.g., Justham et al. 2006), and that this apparent mismatch in effective temperature seems to be a problem for all models, unless the donor stars in short-period BH binaries are pre-main sequence stars (Ivanova 2006). Hence this problem with effective temperatures appears to be a generic problem for models of these systems.

## 5 CONCLUSIONS

In this paper, we have presented a new mechanism for the ejection of a common envelope where the energy source is not orbital energy but nuclear energy. This provides a new channel to produce plausible progenitors of short-period black-hole binaries and long-duration GRBs.

We have also demonstrated that this scenario may be able to explain both the origin and the main properties of short-period black-hole binaries, such as the period distribution, although the distribution of spectral types is still not fully satisfactory.

<sup>10</sup> Note that  $P_{\text{ZAMS}}$  is a function of donor mass, accretor mass and donor radius. Due to angular-momentum loss, the models with initial  $P_{\text{orb}} > P_{\text{ZAMS}}$  have shorter periods by the time they reach contact.

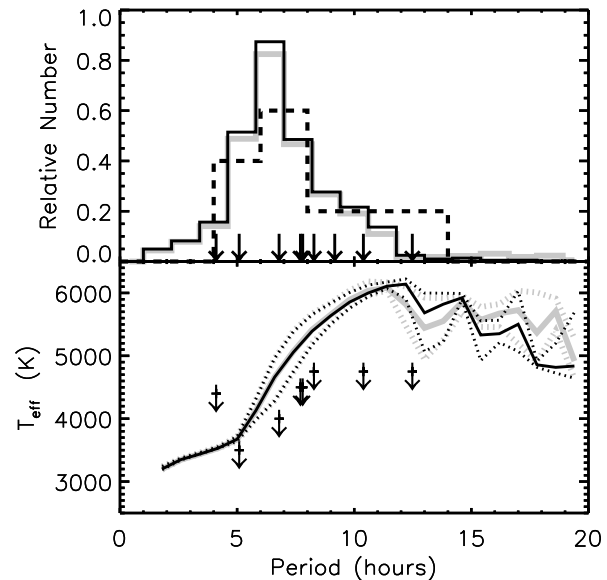


**Figure 4.** Orbital period distribution (upper panel) and distribution of effective temperatures of the secondaries for two population synthesis simulations. The thick grey curves assume a supernova kick dispersion of  $\sigma_k = 200 \text{ km s}^{-1}$ , and the solid black curves correspond to no kick. Both simulations assume a flat initial mass ratio distribution ( $p(q) \propto 1$ ) (changing this to  $p(q) \propto q$  makes little difference to the shape of the distribution, but changes the overall normalisation). In the top panel, the dashed curve represents a histogram of the orbital periods of known systems (also marked with arrows). The normalisation of the histogram of observed systems is arbitrary. The shapes of the period distributions are reasonably well matched. The lower panel shows the median effective temperature (solid curves) and upper and lower quartiles (broken curves) of the populations as a function of orbital period. We also mark the maximum effective temperatures consistent with the spectral types of the known systems (crosses with arrows).

Two of the most attractive features of the explosive CE ejection scenario are that (1) it leads to the ejection of both the hydrogen and the helium layer, explaining why all LGRB supernovae to-date have been classified as Type Ic supernovae, and (2) this ejection occurs late in the evolution of the star; hence the progenitor will only experience a short Wolf-Rayet phase, in which it will not be spun down significantly by wind mass loss. This may also explain why extended Wolf-Rayet wind bubbles are not being found around LGRBs; e.g., in the case of GRB 021004, van Marle, Langer & Garcia-Segura (2005) found that the Wolf-Rayet phase had to last less than  $10^4 \text{ yr}$ ; this is consistent with the explosive CE-ejection scenario, since it always requires late case C mass transfer. This also predicts that such Wolf-Rayet bubbles are terminated by a dense shell from the ejected common envelope. Our rate estimate for this channel ( $\sim 10^{-6} \text{ yr}^{-1}$ ) implies that this can produce a significant fraction of all LGRBs; this rate should be higher at lower metallicity, because case C mass transfer is expected to be more common at lower metallicity. Unlike some of the single-star progenitor models for LGRBs (Yoon & Langer 2005; Woosley & Heger 2006; Yoon, Langer &



Norman 2006), LGRBs may occur even at solar metallicity, but they are expected to be more common at low metallicity. Indeed, there is some evidence now that LGRBs can also occur in super-solar host galaxies (see, e.g., Levesque et al. 2010). The different metallicity biases may provide a possible way of distinguishing between these two different scenarios.

Explosive CE ejection also operates for lower-mass primaries that are expected to produce neutron stars rather than black holes. It is tempting to associate these with rapidly rotating neutron stars and possibly magnetars, for which SN 2006aj, which was associated with the X-ray flash GRB 060218, may provide an observed example in nature (Mazzali et al. 2006).

## ACKNOWLEDGEMENTS

NI gratefully acknowledges support from the NSERC of Canada and from the Canada Research Chairs Program. SJ is partially supported by the National Science Foundation of China under grant numbers 10903001 and 10950110322, and by the Chinese Postdoc Fund (award number 20090450005).

## REFERENCES

- Akiyama S., Wheeler J. C., Meier D. L., Lichtenstadt I., 2003, *ApJ*, 584, 965
- Alexander D. R., Ferguson J. W. 1994, *ApJ*, 437, 879
- Beer H., Voss, F., Winters, R. R., 1992. *ApJS*, 80, 403
- Beer M. E., Podsiadlowski Ph., 2002, *MNRAS*, 331, 351
- Belczynski K., et al., 2008, *ApJS*, 174, 223
- Brandt W. N., Podsiadlowski Ph. 1995, *MNRAS*, 274, 461
- Brandt W. N., Podsiadlowski Ph., Sigurdsson S., 1995, *MNRAS*, 277, L35
- Brown G. E., Lee C.-H., Wijers R. A. M. J., Lee H. K., Israelian G., Bethe H. A., 2000, *NewA*, 5, 191
- Brown G. E., Lee C.-H., Moreno Méndez E., 2007, *ApJ*, 671, L41
- Bucciantini N., Quataert E., Arons J., Metzger B.D., Thompson T. A., 2008, *MNRAS*, 383, L25
- Burrows A., Dessart L., Livne E., Ott C. D., Murphy J., 2007, *ApJ*, 664, 416
- Cannon R., 1993, *MNRAS*, 263, 817
- Cappellaro E., Evans R., Turatto M. 1999, *A&A*, 351, 459
- Detmers R. G., Langer N., Podsiadlowski, Ph., Izzard R. G., 2008, *A&A*, 484, 831
- Dewi J., Tauris T., 2001, in Podsiadlowski Ph., Rappaport, S., King A. R., D'Antona F., Burderi L., eds, *ASP Conf. Ser. Vol. 229, Evolution of Binary and Multiple Star Systems. Astron. Soc. Pac., San Francisco*, p. 225
- Eggleton P. P., 1971, *MNRAS*, 151, 351
- Eggleton P. P., Verbunt F., 1986, *MNRAS*, 220, 13
- Foellmi C., Dall T. H., Depagne E., 2007, *A&A*, 464, 61
- Fruchter A. S., et al., 2006 *Nat* 441, 463
- Fryer C. L., Kalogera V., 2001, *ApJ*, 554, 548
- Fullerton A. W., Massa D. L., Prinja R. K., 2006, *ApJ*, 637, 1025
- González Hernández J. I., Rebolo R., Israelian G., 2008, *A&A*, 478, 203
- Heger A., Langer N., 1998, *A&A*, 334, 210
- Heger A., Woosley S. E., Spruit H. C., 2005, *ApJ*, 626, 350
- Hobbs G., Lorimer D. R., Lyne A. G., Kramer M., 2005, *MNRAS*, 360, 974
- Hurley, J. R., Pols, O. R., Tout, C. A., 2000, *MNRAS*, 315, 543
- Israelian G., Rebolo R., Basri G., Casares J., Martin E. L., 1999, *Nat*, 401, 142
- Ivanova N., 2002, *DPhil Thesis (Oxford)*
- Ivanova N., 2006, *ApJ*, 653, L137
- Ivanova N., Kalogera V., 2006, *ApJ*, 636, 985
- Ivanova N., Podsiadlowski Ph., 2003, in W. Hillebrandt, B. Leibundgut, eds, *From Twilight to Highlight: the Physics of Supernovae*. Springer, Berlin, p. 19
- Ivanova N., Podsiadlowski Ph., 2010, in preparation
- Ivanova N., Podsiadlowski Ph., Spruit H., 2002, *MNRAS*, 334, 819
- Ivanova N., Taam R. E., 2003, *ApJ*, 599, 516
- Justham S., Rappaport S., Podsiadlowski Ph., 2006, *MNRAS*, 366, 1415
- Justham S., Podsiadlowski Ph., 2010, in preparation
- Kalogera V., 1996, *ApJ*, 471, 352
- Kippenhahn R., Weigert A., Hofmeister E., 1967, in Alder B., Fernbach S., Rothenberg M., eds, *Methods in Computational Physics*, Vol. 7. Academic, New York, p. 129
- Kobulnicky H. A., Fryer C. L., 2007, *ApJ*, 670, 747
- Kroupa P., Tout C. A., Gilmore G., 1993, *MNRAS* 262, 545
- Lauterborn D., 1970, *A&A*, 7, 150
- Lee C.-H., Brown G. E., Wijers R. A. M. J., 2002, *ApJ*, 575, 996
- Levesque E. M., Kewley L. J., Graham J. F., Fruchter A. S., 2010, *ApJL*, 712, L26
- MacFadyen A. I., Woosley S. E., 1999, *ApJ*, 524, 262
- Mazzali P., et al., 2006, *Nat*, 442, 1018
- Meyer F., Meyer-Hofmeister E., 1979, *A&A*, 78, 167
- Modjaz M., et al., 2008, *AJ*, 135, 1136
- Moffat A. F. J., Carmelle R., 1994, *ApJ*, 421, 310
- Newman, M., 1978. *ApJ*, 219, 676
- Nieuwenhuijzen H., de Jager C., 1990, *A&A*, 231, 134
- Paczynski B. 1976, in Eggleton, P. P., Mitton S., Whelan J., eds, *Structure and Evolution in Close Binary Systems*. Dordrecht, Reidel, p. 75
- Pfahl E., Rappaport S., Podsiadlowski Ph., 2003, *ApJ*, 597, 1036
- Podsiadlowski Ph., 2001, in Podsiadlowski Ph., Rappaport S., King A. R., D'Antona F., Burderi L., eds, *ASP Conf. Ser. Voll 229, Evolution of Binary and Multiple Star Systems. Astron. Soc. Pac., San Francisco*, p. 239
- Podsiadlowski Ph., Cannon R. C., Rees M. J., 1995, *MNRAS*, 274, 485
- Podsiadlowski Ph., Mazzali P. A., Nomoto K., Lazzati D., Cappellaro E., 2004, *ApJ*, 607, L17
- Podsiadlowski Ph., Nomoto K., Maeda K., Nakamura T., Mazzali P., Schmidt B., 2002, *ApJ*, 567, 491
- Podsiadlowski Ph., Rappaport S., Han Z., 2003, *MNRAS*, 341, 385 (PRH)
- Podsiadlowski Ph., Rappaport S., Pfahl E., 2002, *ApJ*, 565, 1107
- Pols O. R., Tout C. A., Eggleton P. P., Han Z., 1995, *MNRAS*, 274, 964
- Pols O. R., Tout C. A., Schröder K.-P., Eggleton P. P., Manners J., 1997, *MNRAS*, 289, 869
- Rogers F. J., Iglesias C. A. 1992, *ApJS*, 79, 507
- Romani R. W., 1998, *A&A*, 333, 583
- Schröder K.-P., Pols O. R., Eggleton P. P. 1997, *MNRAS*, 285, 696
- Siess L., Livio M. 1999a, *MNRAS*, 304, 925
- Siess L., Livio M. 1999b, *MNRAS*, 308, 1133
- Thielemann F.-K., Truran J. W., Arnould M., 1986, in *Advances in nuclear astrophysics*, Frontieres, Gif-sur-Yvette, p. 525
- Thompson C. Duncan R. C., 1993, *ApJ*, 408, 194
- Uzdensky D. A., MacFadyen A. I., 2007, *ApJ*, 669, 546
- van Marle A. J., Langer N., Garcia-Segura G., 2005, *A&A*, 444, 837
- Wheeler J. C., Yi I., Höflich P., Wang L., 2000, *ApJ*, 537, 810
- Wijers R. A. M. J., 1996 in Wijers R. A. M. J., Davies M. B., Tout C. A., eds, *Evolutionary Processes in Binary Stars*. Kluwer, Dordrecht, p. 327
- Wolf C., Podsiadlowski Ph., 2007, *MNRAS*, 375, 1049
- Woosley S. E., 1993, *ApJ*, 405, 273



- Woosley S. E., Heger A., 2006, ApJ, 637, 914  
Yoon S.-C., Langer N., 2005, A&A, 443, 643  
Yoon S.-C., Langer N., Norman C., 2006, A&A, 460, 199  
Yungelson L. R., Lasota J.-P., Nelemans G., Dubus G., van den  
Heuvel E. P. J., Dewi J., Portegies Zwart S., 2006, A&A, 454,  
559